

Crystal Structure, Infrared Spectra and Density Functional Theory Study on 2,3-Diketo-benzopiperazine Dimer

by P.S. Zhao^{1*}, F.F. Jian^{2*}, H.L. Xiao² and P.P. Sun²

¹Department of Chemistry, Huaiyin Teachers' College, Huaian, Jiangsu, 223001, P.R. China

²New Materials & Function Coordination Chemistry Laboratory,
Qingdao University of Science and Technology, Qingdao Shandong 266042, China
E-mail: ffj2003@163169.net

(Received April 15th, 2004; revised manuscript May 18th, 2004)

2,3-Diketo-benzopiperazine, which exists as dimeric form in its crystal structure has been synthesized. The calculated results on the dimer at B3LYP/6-31G* level show that the average strength of the double hydrogen bonds is of medium-grade. Natural bond orbital analyses have been performed. The predicted harmonic vibration frequencies support the experimental values. The thermodynamic properties of the dimer at different temperatures have been calculated and the change of Gibbs free energy for the aggregation from the monomer to the dimer $\Delta G_T = -30.86$ kJ/mol at 298.15 K, which implies the spontaneous process of the dimer formation.

Key words: 2,3-diketo-benzopiperazine, dimer, crystal structure, density functional theory, thermodynamic property

The importance of hydrogen-bonded dimers has become apparent in the last decade. Hydrogen bond interactions are known to play an important role in determining the structure of molecular crystals and biological systems [1–3]. This has prompted experimentalists [4–5], as well as theoreticians [6–7], to focus their attention on these small systems. Density functional theory (DFT) has long been recognized as a better alternative tool in the study of organic chemical systems, than the *ab initio* methods used in the past [8], due to the fact that it is computationally less demanding for inclusion of electron correlation. Detailed analyses [9–10] on the performance of different DFT methods had been carried out, particularly for equilibrium structure properties of molecular systems. The general conclusion from these studies was, that DFT methods, particularly those with the use of nonlocal exchange-correlation functionals, can predict accurate equilibrium structure properties. The suitability of DFT for reliably describing hydrogen-bonded systems' has been the subject of many investigations [11] and has proved quite useful for studying hydrogen-bonded complexes [7].

* Author for correspondence.

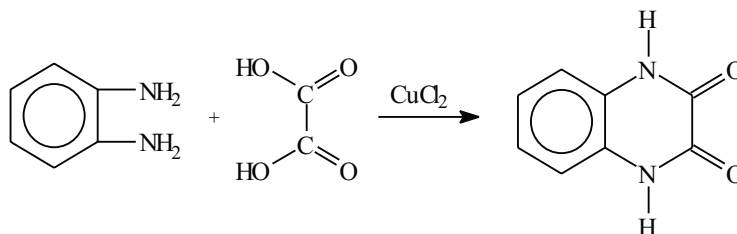
With these in mind, when we synthesized 2,3-diketo-benzopiperazine and found that 2,3-diketo-benzopiperazine exists as dimeric form in the crystal structure, we chose to carry out DFT calculations on this dimer. To the best of our knowledge, the supramolecular structures connected through double, triple or quadruple hydrogen-bonds are difficult to analyze [3] and the crystal structures analyses have been proved to be useful methods. Herein, we report the crystal structure, FTIR spectra and the DFT calculations of the 2,3-diketo-benzopiperazine dimer.

COMPUTATIONAL AND EXPERIMENTAL METHODS

Computational methods. All calculations were performed with Gaussian 98 software package [12] on Pentium IV computer, using the default convergence criteria. Density functional calculations were all self-consistent Kohn-Sham calculations, using the B3LYP density functional. B3LYP combines the exchange functional of Becke's three-parameters [13] with the correlation functional proposed by Lee, Yang, and Parr [14]. In terms of disk space, computer time and the size of the molecules studied here, the standard 6-31G* Gaussian basis set, due to Binkley and Pople *et al.* [15–16], was used for B3LYP density functional calculation. Geometry optimizations were performed using the Berny gradient optimization method [17]. Vibrational frequencies calculated ascertain the structure to be the stable, (no imaginary frequencies). Basis set superposition errors (BSSE) were accounted for by employing the Boys-Bernardi's counterpoise procedure (CP) [18–20]. Natural bond orbital analyses [21] were performed on the optimized structure.

Synthesis. All chemicals were obtained from a commercial source and used without further purification. An ethanol solution (20 mL) of *o*-diaminobenzene (0.54 g, 5.0 mmol) and oxalic acid (0.450 g, 5.0 mmol) are mixed, and the aqueous solution (15 mL) of CuCl_2 (0.336 g, 0.25 mmol) was added in with stirring, then the mixture was sealed in a 50 mL stainless-steel reactor with Teflon liner at 110°C for 48 h, resulting in the formation of the colorless crystals of 2,3-diketo-benzopiperazine. Yield: 85%. Anal. Calcd. for $\text{C}_8\text{H}_6\text{N}_2\text{O}_2$: C, 59.24; H, 3.73; N, 17.28. Found: C, 59.01; H, 3.52; N, 17.06.

The synthesis pathway of 2,3-diketo-benzopiperazine is shown in Scheme 1.



Scheme 1. Synthesis pathway of 2,3-diketo-benzopiperazine.

X-ray structure determination. The selected crystal of 2,3-diketo-benzopiperazine was mounted on a Rigaku Raxis-IV diffractometer. Reflection data were measured at 20°C, using graphite monochromated $\text{Mo-K}\alpha$ ($\lambda = 0.71073 \text{ \AA}$) radiation. The collected data were reduced by using the program SAINT [22]. The structure was solved by direct methods and refined by full-matrix least-squares method on F_{obs}^2 by using the SHELXTL software package [23]. All non-H atoms were anisotropically refined. The hydrogen atom positions were fixed geometrically at calculated distances and allowed to ride on the parent carbon atoms. The final least-square cycle gave $R = 0.0623$, $R_w = 0.1535$ for 671 reflections with $I > 2\sigma(I)$; the weighting scheme, $w = 1/[\sigma^2(F_o^2) + (0.0867P)^2]$, where $P = (F_o^2 + 2F_c^2)/3$. Atomic scattering factors and anomalous dispersion corrections were taken from International Tables for X-Ray Crystallography [24]. A summary of the key crystallographic information is given in Table 1.

Table 1. Summary of crystallographic results for the title compound.

Empirical formula	C ₁₆ H ₁₂ N ₄ O ₄
Formula weight	162.15
Temperature	293(2) K
Wavelength	0.71073 Å
Crystal system, space group	Monoclinic, <i>P</i> 2 ₁ / <i>c</i>
Unit cell dimensions	<i>a</i> = 8.0497(16) Å, <i>b</i> = 4.2859(9) Å, <i>c</i> = 20.995(6) Å <i>β</i> = 102.14(3)°
Volume	708.1(3) Å ³
Z, Calculated density	2, 1.521 Mg/m ³
Absorption coefficient	0.113 mm ⁻¹
<i>F</i> (000)	336
<i>θ</i> range for data collection	1.98 to 27.60°
Limiting indices	0 ≤ <i>h</i> ≤ 10, −5 ≤ <i>k</i> ≤ 5, −26 ≤ <i>l</i> ≤ 24
Reflections collected / unique	1812/1128 [<i>R</i> _{int} = 0.1000]
Completeness to <i>θ</i> = 27.51°	68.2%
Refinement method	Full-matrix least-squares on <i>F</i> ²
Data/restraints/parameters	1128/0/110
Goodness-of-fit on <i>F</i> ²	0.988
Final <i>R</i> indices [<i>I</i> > 2σ(<i>I</i>)]	<i>R</i> 1 = 0.0623, <i>wR</i> 2 = 0.1535
<i>R</i> indices (all data)	<i>R</i> 1 = 0.1288, <i>wR</i> 2 = 0.1749
Largest diff. peak and hole	0.265 and −0.316 e Å ⁻³

RESULTS AND DISCUSSION

Total energies and interaction energies. The calculated total energies and interaction energies for the title compound are given in Table 2 along with zero-point energies (ZPE) and BSSE values. The scaling factor for vibrational frequencies is 0.96 [25].

Table 2. Energies of the monomer and the dimer ^a.

	<i>E</i>	ZPE	BSSE	<i>ΔE</i>	<i>ΔE</i> _{C, ZPEc}
monomer	−1491026.66	351.14			
dimer	−2982137.05	707.68	16.33	−83.74	−62.23

^a*E* is the total energy; *ΔE* is the uncorrected interaction energy; *ΔE*_{C, ZPEc} is the interaction energy corrected for BSSE and ZPE.

With BSSE and ZPE corrections, the total energy of the dimer is much lower than the sum of energies of two monomers by 62.23 kJ/mol, which suggests the dimer can be subsistent and the average per hydrogen bond energy is about 31.12 kJ/mol. This hydrogen bond energy is of medium-grade compared with those reported before (8–54 kJ/mol) [2]. The proportions of BSSE to the corrected interaction energies $E_{C, ZPEc}$ are 26.25%, which indicates the BSSE correction for the interaction energies is necessary.

Crystal structures and optimized geometries. The displacement ellipsoid plot with the numbering scheme for the title compound shown in Figure 1 and Figure 2 gives a perspective view of the crystal packing in the unit cell. Atomic parameters and equivalent isotropic thermal parameters of non-H atoms for the title compound are given in Table 3. Selected bond lengths, bond and torsion angles by X-ray diffraction along with calculated values are listed in Table 4.

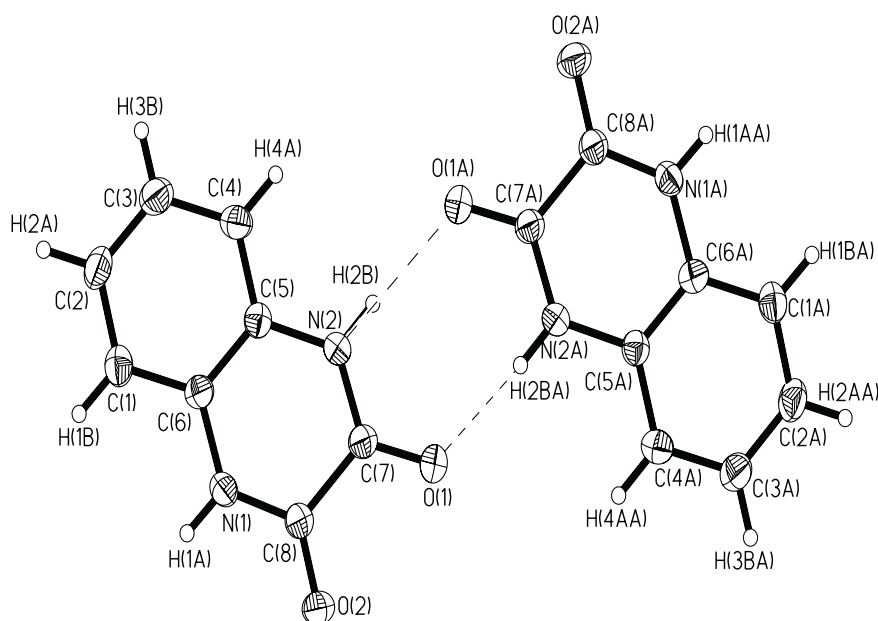


Figure 1. Molecular structure with the atomic numbering scheme for the title compound.

The crystal lattices of 2,3-diketo-benzopiperazine comprise two dimer molecules in the unit cell. Each symmetric dimer molecule consists of two 2,3-diketo-benzopiperazine monomers and the two monomers are connected by double hydrogen bonds. The double hydrogen bonds are $N(2)–H(2B) \cdots O(1A)$ and $N(2A)–H(2BA) \cdots O(1)$, with the separation distances of $N(2) \cdots O(1A)$ and $N(2A) \cdots O(1)$ being equal to 2.8413 Å and the hydrogen bond angles being 172.49°. Bond lengths and angles in the phenyl

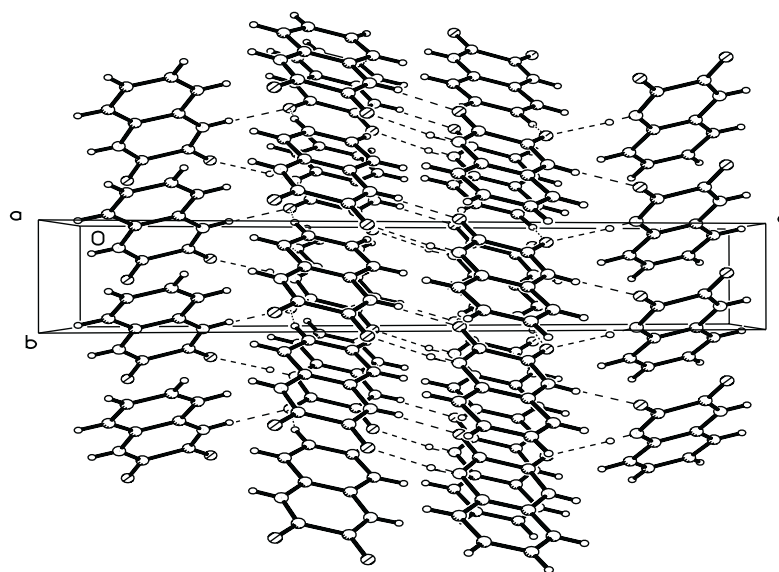


Figure 2. A view of the crystal packing down the *a* axis for the title compound.

ring are generally normal. The bond lengths of N–C (1.333–1.394 Å) are all shorter than the typical N–C single bond distance (1.4685 Å), indicating that the N–C bonds have some character of double bonds. In each monomer, all the non-H atoms except O(1) atom define a plane with the largest deviation 0.032 Å.

Table 3. Atomic coordinates ($\times 10^4$) and equivalent isotropic displacement parameters ($\text{\AA}^2 \times 10^3$).

Atom	<i>x</i>	<i>y</i>	<i>z</i>	<i>U</i> _{eq}	Atom	<i>x</i>	<i>y</i>	<i>z</i>	<i>U</i> _{eq}
O(1)	−1156(3)	5340(7)	634(1)	54(1)	C(3)	4828(5)	−2929(10)	901(2)	57(1)
O(2)	−1229(3)	3195(7)	1870(1)	55(1)	C(4)	3568(4)	−963(9)	586(2)	50(1)
N(1)	1073(3)	203(7)	1838(1)	42(1)	C(5)	2325(4)	78(9)	906(2)	39(1)
N(2)	1080(3)	2178(7)	615(1)	43(1)	C(6)	2341(4)	−915(8)	1536(2)	39(1)
C(1)	3593(4)	−2940(9)	1847(2)	48(1)	C(7)	−127(4)	3376(9)	898(2)	42(1)
C(2)	4838(4)	−3898(10)	1527(2)	54(1)	C(8)	−145(4)	2233(9)	1583(2)	42(1)

*U*_{eq} is defined as one third of the trace of the orthogonalized *U*_{ij} tensor.

In the dimer crystal lattice, there exists one intermolecular hydrogen bond, potentially weak (C–H \cdots Y hydrogen bonds, Y = O) [26–27] intermolecular interactions, and π – π stacking interactions [28–29]. The intermolecular hydrogen bond is N(1)–H(1A) \cdots O(2) (symmetry code: $-X, -1/2+Y, 1/2-Z$), with the donor and acceptor distance 2.8413 Å. The O(2) atom with C(2) atom form potentially weak C–H \cdots O in-

tramolecular interactions and the donor and acceptor distance is 3.3344 Å. There are two types π - π stacking interactions: piperazine ring (X, Y, Z) – phenyl ring ($X, 1+Y, Z$) and phenyl ring (X, Y, Z) – piperazine ring ($X, -1+Y, Z$). The center-to-center distances are all 3.574 Å. The shortest interplanar distances above are 3.308 and 3.324 Å, respectively. In the solid state, all above extensive hydrogen bonds in this structure connected the dimer forms hydrogen bonds networks, which stabilize the dimer crystal structure.

Table 4. Selected structural parameters by X-ray and theoretical calculations.

Bond lengths (Å)	Exp.	Calc.	Bond angles (°)	Exp.	Calc.
O(1)–C(7)	1.226(4)	1.233	C(8)–N(1)–C(6)	125.9(3)	126.3
O(2)–C(8)	1.230(4)	1.216	C(7)–N(2)–C(5)	125.0(3)	125.6
N(1)–C(8)	1.333(4)	1.380	C(4)–C(3)–C(2)	120.0(3)	120.2
N(1)–C(6)	1.394(4)	1.396	C(6)–C(5)–N(2)	118.7(3)	118.6
N(2)–C(7)	1.343(4)	1.360	C(6)–C(5)–C(4)	120.0(3)	120.1
N(2)–C(5)	1.387(4)	1.396	N(2)–C(5)–C(4)	121.2(3)	121.3
C(1)–C(2)	1.380(5)	1.392	C(1)–C(6)–C(5)	120.1(3)	119.9
C(1)–C(6)	1.382(4)	1.398	C(1)–C(6)–N(1)	122.0(3)	122.4
C(2)–C(3)	1.375(5)	1.399	C(5)–C(6)–N(1)	117.9(3)	117.8
C(3)–C(4)	1.374(5)	1.392	O(1)–C(7)–N(2)	122.9(3)	123.2
C(4)–C(5)	1.391(5)	1.399	O(1)–C(7)–C(8)	120.4(3)	120.0
C(5)–C(6)	1.386(4)	1.405	N(2)–C(7)–C(8)	116.6(3)	116.8
C(7)–C(8)	1.522(5)	1.529	O(2)–C(8)–N(1)	123.9(3)	122.9
			O(2)–C(8)–C(7)	120.3(3)	122.2
			N(1)–C(8)–C(7)	115.8(3)	114.9

Seen from Table 4, most of the optimized bond lengths are slightly larger than the experimental values. The theoretical calculations belong to isolated molecules in gaseous phase at 0 K and the experimental results belong to molecules in solid phase. The largest deviations of bond lengths and angles between the theoretical and experimental geometry are 0.041 Å and 1.9°, indicating that the calculational precision is satisfying [30] and the B3LYP/6-31G* level is suitable for the system studied here.

Atomic charges and charge transfer. The Mulliken atomic charges of the monomer and the dimer are listed in Table 5. (Only half of the atoms are listed in view of the symmetry).

Table 5. Atomic charges (in e) of the monomer and the dimer at B3LYP/6-31G* level.

Atom	monomer	dimer	Atom	monomer	dimer
O(1)	-0.4697	-0.5317	C(6)	0.3633	0.3647
O(2)	-0.4697	-0.4777	C(7)	0.5637	0.5700
N(1)	-0.7549	-0.7540	C(8)	0.5637	0.5728
N(2)	-0.7549	-0.7808	H(1A)	0.3413	0.3413
C(1)	-0.1881	-0.1884	H(2A)	0.1405	0.1392
C(2)	-0.1362	-0.1346	H(4A)	0.1402	0.1786
C(3)	-0.1362	-0.1374	H(1B)	0.1402	0.1375
C(4)	-0.1881	-0.1972	H(2B)	0.3414	0.4102
C(5)	0.3633	0.3448	H(3B)	0.1406	0.1426

The charges redistribution mainly occurs among the atoms involved in hydrogen bonds, which do not change the symmetry of dimer. The dipole moment of the dimer is 0.0001 Debye.

Natural bond orbital analysis. In order to probe the origin of the interaction, natural bond orbital (NBO) analyses at B3LYP/6-31G* level were performed. The donor and acceptor (here: donor = donor electrons and acceptor = acceptor electrons) of NBO between intermolecules, and their interaction stable energies are collected in Table 6. The stable energies are proportional to the NBO interacting intensities. In symmetric dimer, the O(1) [O(1A)] atom in one monomer donates its first and second lone pair electrons to the N(2A)–H(2BA) [N(2)–H(2B)] antibonds in another monomer and give total stable energies 98.90 kJ/mol.

Table 6. Natural bond orbital interaction and the corresponding stable energy (kJ/mol)^a.

Donor	Acceptor	<i>E</i>
LP(1) O (1)	BD* N(2A) – H (2BA)	31.52
LP(2) O (1)	BD* N(2A) – H (2BA)	67.38
LP(1) O (1A)	BD*N(2) – H (2B)	31.52
LP(2) O (1A)	BD* N(2) – H (2B)	67.38

^aLP means lone pair; BD* represents antibond.

IR spectra. Some calculated harmonic frequencies and infrared intensities are shown in Table 7 and are compared with the experimental data. Vibrational frequencies calculated were scaled by 0.96 [25]. Gauss-view program [Gaussian Inc.] was used to assign the calculated harmonic frequencies. In view of the symmetric character of the dimer, we only describe the assignment in one monomer.

Table 7. Selected vibrational frequencies^a.

Exp.	Calc.	Description	Exp.	Calc.	Description
3414	3436	N(1)–H(1A) str.	1162	1207–1210	C(8)–N(1) str. + C(7)–N(2) str.
3233	3128	N(2)–H(2B) str.	1096	1023–1146	ip phenyl ring C–H def.
1637	1742–1743	C(8)–O(2) str.	948	936–937	oop phenyl ring C–H def.
1617	1688–1705	C(7)–O(1) str.	796	827–828	oop phenyl ring C–H def. +N(2)–H(2B)
1497	1598–1606	phenyl ring skeleton str.			oop def.
1456	1490	ip phenyl ring C–H def.	748	748	C(7)–C(8) str.
1425	1393–1458	ip phenyl ring C–H def. + N(2)–H(2B) ip def. + N(1)–H(1A)ip def.	722	732–733	oop phenyl ring C–H def.
		C(7)–C(8) str. + N(2)–C(7) str. + N(1)–C(8) str.	695	686–696	dimer skeleton def.
1225	1253	C(5)–N(2) str. + C(6)–N(1) str.	625	642	N(1)–H(1A) str.

^aFrequencies in cm^{−1}. Atomic numbering as shown in Figure 1.
str.: stretch; ip: in-plane; oop: out-of-plane; def.: deformation.

The predicted frequencies and the experimental frequencies reveal good agreement, with the difference equal to about 3.0%. The modes of N(2)–H(2B) and C=O stretch vibrations exhibit large red shifts with respect to those in the monomer, accompanied by the increasing of intensities. These phenomena are caused by the formation of the hydrogen bonds in the dimer, which exists in the solid state.

Thermodynamic properties. On the basis of vibrational analysis and statistical thermodynamics, the standard thermodynamic functions: heat capacities ($C_{p,m}^0$), entropies (S_m^0) and enthalpies (H_m^0), were obtained and listed in Table 8.

As seen from the Table 8, the heat capacities, entropies and enthalpies increase at any temperature ranging from 200.00 to 800.00 K. Due to that the intensities of molecular vibration increase, when the temperature increases. For the dimer, the correlations between these thermodynamic properties and temperatures are as follows:

$$C_{p,m}^0 = -14.39628 + 1.37063 T - 6.87163 \times 10^{-4} T^2$$

$$S_m^0 = 333.46976 + 0.99505 T, \quad H_m^0 = -88.11674 + 0.48181 T$$

The intermolecular interaction is an exothermic process. From 200.00 K to 500.00 K, Gibbs free energies $\Delta G_T < 0$, which implies the spontaneous process of the dimer formation. Above 500.00 K, the $\Delta G_T > 0$ demonstrates that the process of the dimer formation is not spontaneous. At 298.15 K the calculated equilibrium constant, based on the equation $\Delta G_T = -RT \ln K_p$, is $2.55 \cdot 10^5$. It reveals that the dimer is the main component at this temperature. Although the above conclusions are based on the

gaseous-phase state structure, they provide useful references for the dimer synthesis under experimental conditions.

Table 8. The thermodynamic properties of the monomer and the dimer at different temperatures ^a.

Structure	<i>T</i> (K)	$C_{p,m}^0$ (J·mol ⁻¹ ·K ⁻¹)	S_m^0 (J·mol ⁻¹ ·K ⁻¹)	H_m^0 (kJ·mol ⁻¹)	ΔS_T (J·mol ⁻¹ ·K ⁻¹)	ΔH_T (kJ·mol ⁻¹)	ΔG_T (kJ·mol ⁻¹)
monomer	200.00	111.08	337.52	13.01			
	298.15	161.97	391.48	26.44			
	400.00	207.99	445.72	45.35			
	500.00	244.58	496.22	68.05			
	600.00	273.51	543.47	94.01			
	700.00	296.48	587.42	122.56			
	800.00	314.98	628.26	153.16			
dimer	200.0	231.56	517.64	26.78	-157.40	-77.59	-46.11
	298.1	332.90	629.20	54.53	-153.76	-76.70	-30.86
	400.0	425.75	740.40	93.31	-151.04	-75.74	-15.32
	500.0	500.11	843.70	139.74	-148.74	-74.71	-0.34
	600.0	559.17	940.31	192.82	-146.63	-73.55	14.43
	700.0	606.15	1030.17	251.17	-144.67	-72.30	28.97
	800.0	644.04	1113.66	313.74	-142.86	-70.93	43.37

^a $\Delta S_T = (S_m^0)_{\text{dimer}} - 2 * (S_m^0)_{\text{monomer}}$; $\Delta H_T = (H_m^0 + E + \text{ZPE})_{\text{dimer}} - 2 * (H_m^0 + E + \text{ZPE})_{\text{monomer}}$; $\Delta G_T = \Delta H_T - T\Delta S_T$ and the scale factor for frequencies is 0.96 [25].

Supplementary material. CCDC-227509 contains the supplementary crystallographic data for this paper. These data can be obtained free of charge at www.ccdc.cam.ac.uk/consts/retrieving.html [or from the Cambridge Crystallographic Data Centre (CCDC), 12 Union Road, Cambridge CB2 1EZ, UK; fax: +44(0)1222-336033; email: deposit@ccdc.cam.ac.uk].

Acknowledgment

This work was supported by Natural Science Research Guidance Project of University in Jiangsu Province (03KJD150053) and Natural Science Foundation of Shandong Province (No.Y2002B06), China.

REFERENCES

1. Jeffrey G.A. and Saenger W., *Hydrogen Bonding in Biological Structures*, Springer-Verlag: Berlin, 1991.
2. Philp D. and Stoddart J.F., *Angew. Chem. Int. Ed. Engl.*, **35**, 1154 (1996).
3. Sherrington D.C. and Taskinen K.A., *Chem. Soc. Rev.*, **30**, 7623 (2001).
4. Legon A.C., *Chem. Soc. Rev.*, **19**, 197 (1990).
5. Steinke J.H.G. and Sherrington D.C., *Trends Anal. Chem.*, **18**, 159 (1999).
6. Scheiner S., *Reviews in Computational Chemistry*, VCH: NY, 1991, Vol. 2, p. 165.
7. Freccero M., Di Valentin C. and Sarzi-Amade M., *J. Am. Chem. Soc.*, **125**, 3544 (2003).
8. Labanowski J.K. and Andzelm J., *Density Functional Methods in Chemistry*. Springer Verlag: NY, 1991.
9. Dickson R.M. and Becke A.D., *J. Chem. Phys.*, **99**, 3898 (1993).
10. Oliphant N. and Bartlett R.J., *J. Chem. Phys.*, **100**, 6550 (1994).
11. Guo H., Sirois S., Proynov E.I. and Salaub D.R., In *Theoretical Treatment of Hydrogen Bonding*; Hadzy, D., Ed.; Wiley: NY, 1997.
12. Frisch M.J., Trucks G.W., Schlegel H.B., Scuseria G.E., Robb M.A., Cheeseman J.R., Zakrzewski V.G., Montgomery A.J., Jr., Stratmann R.E., Burant J.C., Dapprich S., Millam J.M., Daniels A.D., Kudin K.N., Strain M.C., Farkas O., Tomasi J., Barone V., Cossi M., Cammi R., Mennucci B., Pomelli C., Adamo C., Clifford S., Ochterski J., Petersson G.A., Ayala P.Y., Cui Q., Morokuma K., Malick D.K., Rabuck A.D., Raghavachari K., Foresman J.B., Cioslowski J., Ortiz J.V., Baboul A.G., Stefanov B.B., Liu G., Liashenko A., Piskorz P., Komaromi I., Gomperts R., Martin R.L., Fox D.J., Keith T., Al-Laham M.A., Peng C.Y., Nanayakkara A., Gonzalez C., Challacombe M., Gill P.M.W., Johnson B., Chen W., Wong M.W., Andres J.L., Gonzalez C., Head-Gordon M., Replogle E.S. and Pople J.A., *Gaussian 98*, Revision A. 7, Gaussian, Inc., Pittsburgh PA, 1998.
13. Becke A.D., *J. Chem. Phys.*, **98**, 5648 (1993).
14. Lee C., Yang W. and Parr R.G., *Phys. Rev.*, **B37**, 785 (1988).
15. Binkley J.S., Pople J.A. and Hehre W.J., *J. Am. Chem. Soc.*, **102**, 939 (1980).
16. Gordon M.S., Binkley J.S., Pople J.A., Pietro W.J. and Hehre W.J., *J. Am. Chem. Soc.*, **104**, 2797 (1982).
17. Peng C., Ayala P.Y., Schlegel H.B. and Frisch M.J., *J. Comput. Chem.*, **17**, 49 (1996).
18. Boys S.F. and Bernardi F., *Mol. Phys.*, **19**, 553 (1970).
19. Johansson A., Kollman P. and Rothenberg S., *Theor. Chim. Acta*, **29**, 167 (1973).
20. Chalasinski G. and Szczesniak M.M., *Mol. Phys.*, **63**, 205 (1988).
21. Reed A.E., Weinstock R.B. and Weinhold F., *J. Chem. Phys.*, **83**, 735 (1985).
22. Sheldrick G.M., *SAINT v4 Software Reference Manual*, Siemens Analytical X-ray Systems, Inc., Madison, Wisconsin, USA 1996.
23. Sheldrick G.M., *SHELXTL, v5 Reference Manual*, Siemens Analytical X-ray Systems, Inc., Madison, Wisconsin, USA 1996.
24. Wilson A.J., *International Tables for X-ray Crystallography*, Volume C 1992, Kluwer Academic Publishers, Dordrecht: Tables 6.1.1.4 (pp. 500–502) and 4.2.6.8 (pp. 219–222).
25. Pople J.A., Schlegel H.B., Krishnan R., Defrees D.J., Binkley J.S., Frisch M.J., Whiteside R.A., Hout R.F. and Hehre W.J., *Int. J. Quantum Chem., Quantum Chem. Symp.*, **15**, 269 (1981).
26. Steiner T., *Cryst. Rev.*, **6**, 1 (1996).
27. Jeffrey G.A., Maluszynska H.J. and Mitra J., *Int. J. Biol. Macromol.*, **7**, 336 (1985).
28. Glusker J.P., Lewis M.M. and Rossi M., *Crystal structure analysis for chemists and biologists*. VCH Publishers Inc, NY, 1994.
29. Hunter R.H., Hauelsen R.H. and Irving A., *Angew. Chem. Int. Ed. Engl.*, **33**, 566 (1994).
30. Hahre W.J., Radom L., Schleyer P.V.R. and Pople J., *Ab Initio Molecular Orbital Theory*, Wiley, NY, 1986.